THE ASTROPHYSICAL JOURNAL, 413:593–603, 1993 August 20

COMETARY GLOBULES IN THE SOUTHEAST QUADRANT OF THE ROSETTE NEBULA

NIMESH A. PATEL, TAOLING XIE[1], AND PAUL F. GOLDSMITH[2]
Five College Radio Astronomy Observatory, Department of Physics and Astronomy,
University of Massachusetts, Amherst, MA 01003
Received 1992 August 31; accepted 1993 February 25

ABSTRACT

We present a study of newly identified cometary globules in the southeast quadrant of the Rosette nebula using the $J = 1$–0 transition of carbon monoxide. The globules are found to be blueshifted by about 6 km s^{-1} with respect to the adjacent Rosette molecular cloud. The masses of the globules vary from 50 to 300 $M_\odot$, and their sizes are between 1 and 3 pc. Two of the globules have cometary morphology and show velocity gradients of $\sim$1.5 km s^{-1} pc^{-1} along their symmetry axes. These globules are associated with the *IRAS* sources 06314+0421, X0632+043, 06322+0427, and 06327+0423 which coincide with local maxima in the ^{13}CO emission. The derived physical parameters of the globules are found to be consistent with those predicted by recent theoretical models of photoevaporating cometary clouds. We suggest that star formation induced by radiation driven implosion has occurred.

Subject headings: infrared: interstellar: lines — H II regions — ISM: clouds — ISM: individual (NGC 2244) — ISM: molecules

1. INTRODUCTION

Several recent studies have suggested that radiation driven implosion is a significant mechanism for inducing star formation in molecular clumps located in the neighborhood of O stars (Klein, Whitaker, & Sandford 1985; Sugitani et al. 1989; Bertoldi 1989; Bertoldi & McKee 1990; Sugitani, Fukui, & Ogura 1991). These clumps presumably evolve from the projections on the surface of a giant molecular cloud, which are typically convoluted (Dickman, Horvath, & Margulis 1990; Falgarone, Phillips, & Walker 1991). The clumpy structure at the surface of the molecular cloud allows the UV radiation from a neighboring H II region to penetrate deep into the cloud (Stutzki et al. 1988; Boissé 1990; Cox, Deharveng, & Leene, 1990; Tauber & Goldsmith 1990; Goldsmith et al. 1992a; Elmegreen 1992).

If sufficiently intense, the UV flux can have a significant influence on the clumps and result in their taking on a cometary shape, with bright rims roughly facing the direction of the exciting star(s). These bright rims were first noticed by Duncan (1920) and were later studied in detail at optical wavelengths (Pottasch 1956; 1958a, b; Osterbrock 1957; Dibai 1960; Schneider & Elmegreen 1979). An evolutionary sequence based on morphology has been suggested by Reipurth (1983), Leung (1985), and Elmegreen (1992). Sugitani et al. (1991) have recently published an optical catalog of 44 such objects in the northern hemisphere, which are associated with *IRAS* point sources. While these studies reveal the morphological features of the globules and are useful for identifying associated objects, the internal kinematic structure of the globules and their motion with respect to the surrounding interstellar medium, as well as their masses and other properties, can be revealed only by detailed spectral line observations at millimeter wavelengths. Radio observations can also reveal newer globules which may be missed by optical studies due to their having insufficient column density or to the presence of excessive diffuse brightness. However, few such studies have been made so far. The elephant trunk globules in the northwest quadrant of the Rosette nebula have been studied by Schneps, Ho, & Barrett (1980), the cometary globules in IC 1396 by Wootten et al. (1983), Nakano et al. (1989), Duvert et al. (1990), and Serabyn, Güsten, & Mundy (1993), and those in the Gum nebula by Harju et al. (1990), Sahu et al. (1988), and Sridharan (1992).

A well-known example of an H II region showing the presence of speck and elephant trunk globules in the Rosette nebula in Monoceros (NGC 2237-44) which is at a distance of about 1600 pc (Turner 1976). Optical and 4.75 GHz radio continuum emission (Celnick 1985) indicates the presence of ionized gas around the nebula which reaches the boundary of the molecular gas. Cox et al. (1990) have studied the *IRAS* emission from the Rosette nebula and the surrounding molecular cloud. Recently, Kuchar, Blitz, & Bania (1993) have found an expanding H I shell around the Rosette nebula.

Cometary globules have been recently found in the southeast quadrant of NGC 2244 (Block 1990; Block, Dyson, & Madsen 1992; Sugitani et al. 1991). These globules exist near the Rosette molecular complex mapped in ^{12}CO (hereafter CO) and ^{13}CO by Blitz & Thaddeus (1980) and Blitz & Stark (1986). One of the globules shows the presence of a bright rim that roughly faces the cluster of young stars in the Rosette nebula. The exciting stars in NGC 2244 are located northwest of this region at a projected distance of $\sim$25 pc.

Although CO emission has been detected from the region covered by these objects (Blitz & Stark 1986), due to relatively low angular resolution and coarse sampling, the morphology and kinematics of the globules remain unclear. We have surveyed this region with resolution and sampling improved by about a factor of 2 compared to the previous observations. In this paper we report the results obtained from our fully sampled CO and ^{13}CO maps of this region. In the next section we present the observational procedure. In § 3 we give the results, derive the physical conditions in the globules, and discuss their morphology, kinematics, and *IRAS* association.

[1] Also: Jet Propulsion Laboratory, California Institute of Technology.
[2] Also: National Astronomy and Ionosphere Center, Cornell University.

We compare our observational results with some of the theoretical models of cometary globules in § 4 and summarize our conclusions in § 5.

2. OBSERVATIONS

We mapped a 0°.5 × 0°.5 region in CO and ^{13}CO $J = 1–0$ transitions with the FCRAO 14 m telescope at New Salem, Massachusetts, during 1991 October and November. We used the 15-element QUARRY receiver (Erickson et al. 1992) with a set of filter banks each having 32 channels and a velocity resolution of 0.65 km s^{-1} (at 115 GHz) as the primary spectrometer. The typical system temperature (SSB), referred to above Earth's atmosphere, was about 700 K at 115 GHz and about 500 K at 110 GHz. The data were acquired in position-

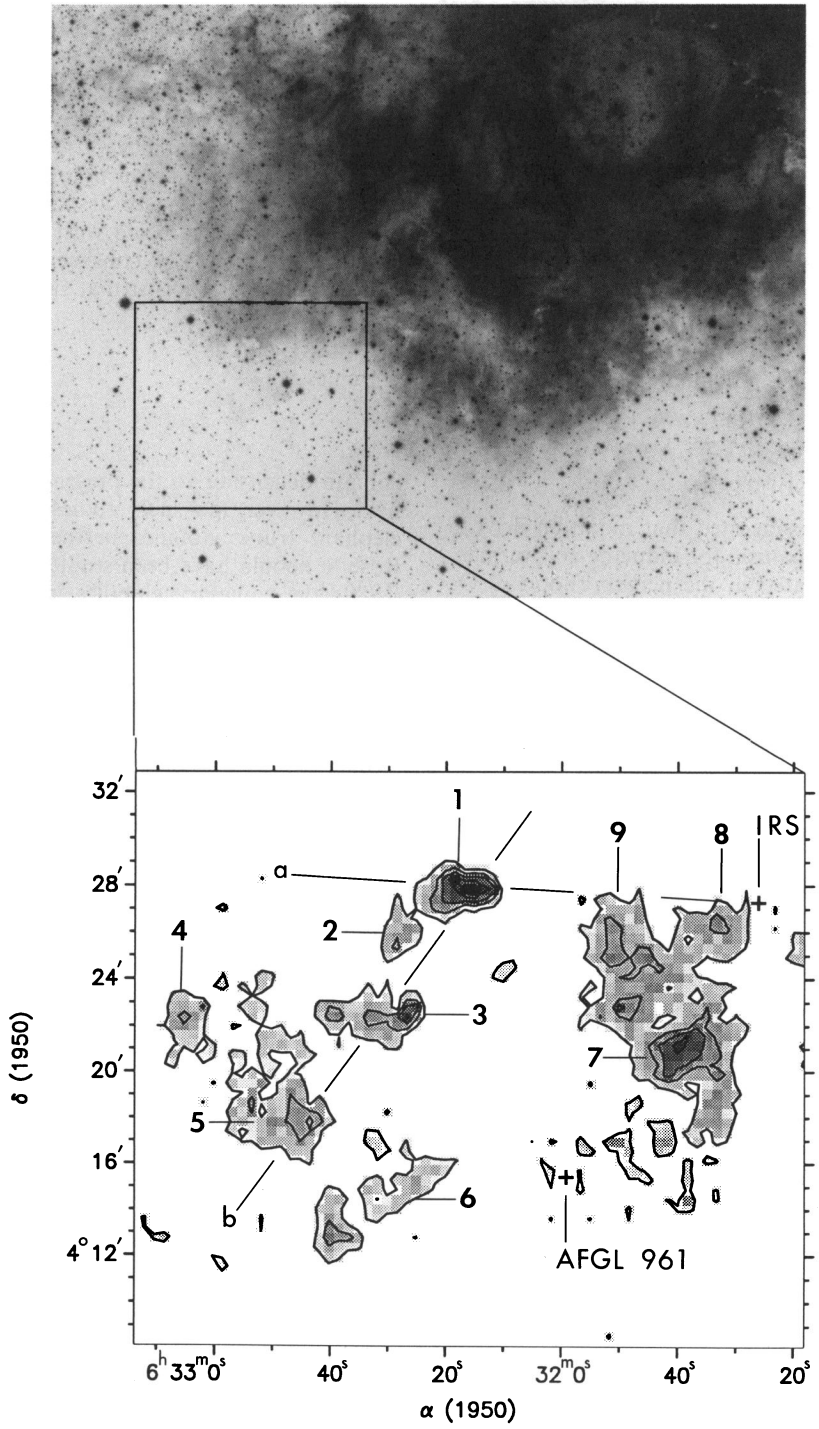

FIG. 1.—A POSS red print of the Rosette nebula and surrounding region. The region we mapped, indicated by the rectangle, is expanded in the lower panel showing the integrated ^{13}CO emission in the velocity range 5–12 km s^{-1}. The contour levels are between 1 and 6 K km s^{-1}, separated by 1 K km s^{-1}. Each gray-shaded box represents a sampled spectrum in the map, with the shading scaled linearly with the integrated intensity. The globules we have identified are labeled in this figure. On a large scale, the molecular emission is anticorrelated with the optical brightness which represents ionizing radiation. Globule 3 is not visible in optical extinction, while the three cometary globules detected in the masked photographs by Block (1990) are not evident in CO emission.

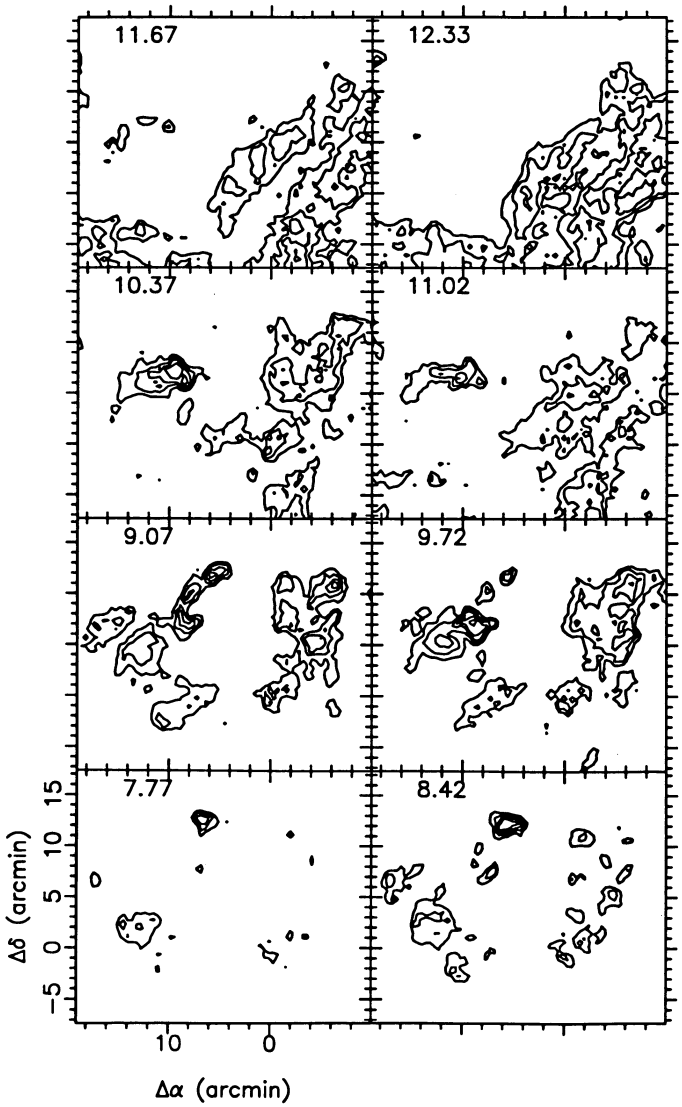

FIG. 2a

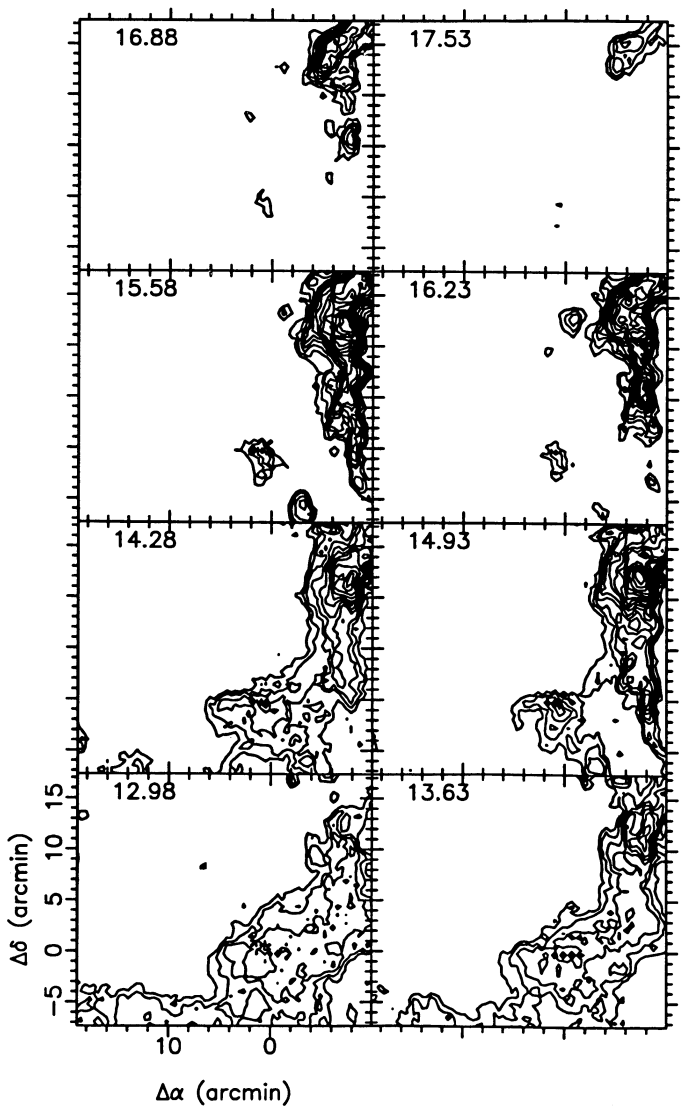

FIG. 2b

FIG. 2.—Channel maps of CO emission. The contour levels are separated by 1 K between 2 and 16 K. The globules appear at velocities 8–12 km s^{-1} while the stronger emission from the Rosette cloud appears at 14–17 km s^{-1}. At ($\Delta\alpha$, $\Delta\delta$) = (0′, 0′), we note the emission from the AFGL 961 outflow with the redshifted lobe at around 15 km s^{-1} and the blueshifted lobe at around 9 km s^{-1}; the bipolarity of the outflow is evident even at low velocities. At (7′, 11′), the fragmentation of globule 1 is seen clearly at 9 km s^{-1}.

switching mode with the reference position at $\alpha(1950) = 06^h37^m43^s.8$, $\delta(1950) = 04°43'08''$ (Blitz & Stark 1986), and calibration was achieved using a chopper-wheel. The pointing and gain calibration were checked by observing SiO maser sources and planets. The rms pointing error was about 5″ and the main beam efficiency was estimated to be ~0.45 at both frequencies.

AFGL 961, located at $\alpha(1950) = 06^h31^m58^s$, $\delta(1950) = +04°15'30''$ (Blitz & Thaddeus 1980), is the central position in the CO and ^{13}CO maps. The spacing of the data points is 25″ and the half-power beamwidth is about 45″ at 115 GHz. At the distance of Rosette, 1′ is equivalent to 0.47 pc. The rms noise in each channel is typically 0.2 K in CO and 0.1 K in ^{13}CO.

3. RESULTS

3.1. *Morphology and Kinematics*

Figure 1 shows the POSS red print of the southeast quadrant of the Rosette nebula together with a map of integrated ^{13}CO emission. Figures 2 and 3 show the channel maps of CO and ^{13}CO emission, respectively. The optical emission in Figure 1 corresponds mostly to the ionizing radiation from the central stars in the Rosette nebula, and it appears to be anticorrelated with the CO emission. The lack of CO emission from the region around (α, δ) = ($06^h32^m10^s$, 04°22′) in Figure 1, or ($\Delta\alpha$, $\Delta\delta$) = (5′, 5′) in Figures 2 and 3, is presumably due to the dissociation of molecules by UV radiation which has penetrated relatively deeply into the edge of the molecular cloud. The presence of a rich velocity structure in this region is evident from the channel maps. We see that the globules appear in the velocity range between 8 and 12 km s^{-1}, while the stronger extended emission exists between velocities of 12 and 17 km s^{-1}. In Figure 1, the ^{13}CO emission is integrated between 5 km s^{-1} and 12 km s^{-1}. The corresponding map of integrated CO emission appears similar to that shown in Figure 1, in which the globules are identified and labeled. The stronger extended emission shown in Figures 2*b* and 3*b* corre-

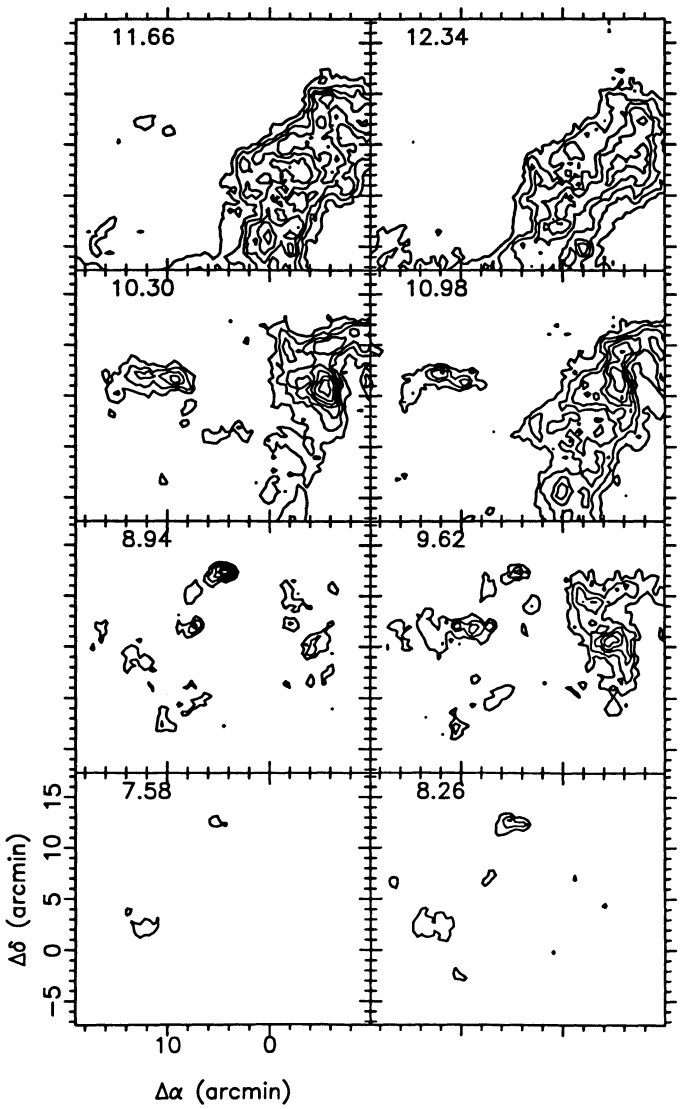

FIG. 3a

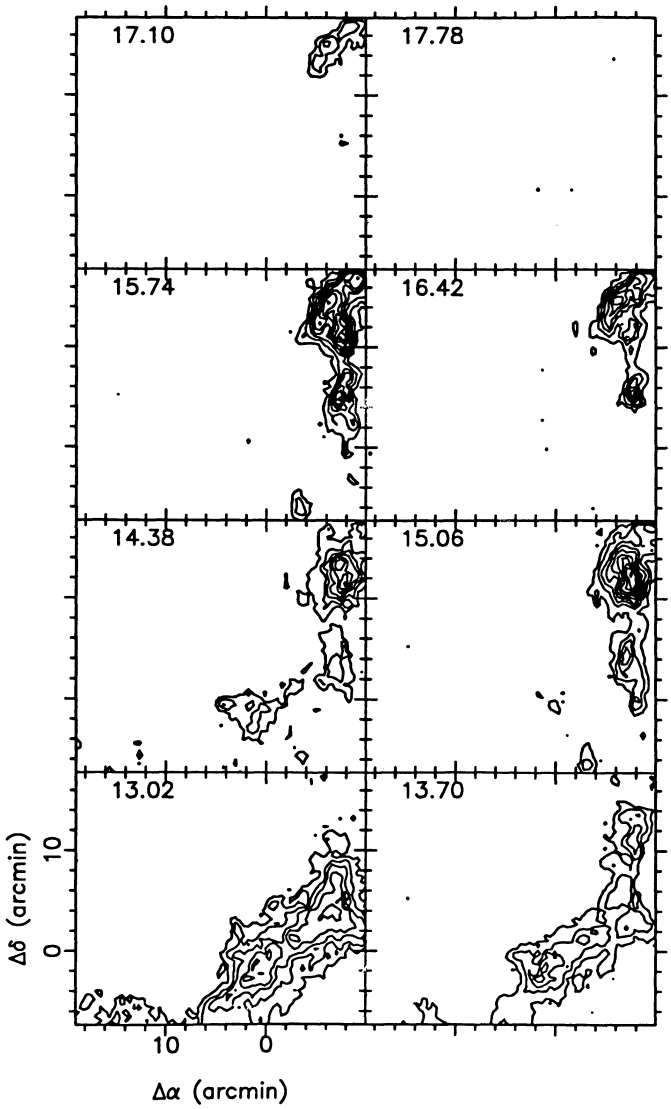

FIG. 3b

FIG. 3.—Channel maps of ^{13}CO emission. The contour levels are separated by 0.5 K between 0.5 and 6 K.

sponds to the region of strongest emission in the Rosette molecular cloud which was mapped by Blitz & Thaddeus (1980). It is clear from Figures 2*a* and 2*b* that the globules are blueshifted by 6–7 km s^{-1} with respect to the Rosette cloud. Since objects 1–6 appear relatively well isolated, we refer to them as globules. Objects 7–9 (clumps) appear to be superposed over the emission from the Rosette cloud, but they have the same velocity as the globules.

In Figure 2*b*, the peak in CO antenna temperature appears at ~ 15 km s^{-1} at $(\Delta\alpha, \Delta\delta) = (-7', 12')$. Blitz & Thaddeus (1980) found this location to be the peak in CO emission throughout the Mon OB2 complex. This peak coincides with the location of IRAS 06314+0427 (Cox et al. 1990; Block 1990). We refer to this source hereafter as IRS (note that Blitz & Thaddeus refer to AFGL 961 as "IRS").

At the location of AFGL 961, Blitz & Thaddeus (1980) found CO emission to be self-absorbed, in a region roughly elongated toward the northwest with an extension of about 1 pc × 3 pc. From Figure 2*a*, at 11 and 11.7 km s^{-1}, there appears a lack of CO emission in a narrow region passing through the location of AFGL 961 and inclined toward the northwest; while in Figure 3*a*, the ^{13}CO emission appears continuous in this region at these velocities. Thus, we see that the region over which CO self-absorption occurs is significantly larger than was indicated by Blitz & Thaddeus (1980). When compared to the ^{13}CO emission, the absorption dip in CO line profiles is slightly blueshifted. Self-reversed profiles are seen from a few other regions in giant molecular clouds (Snell & Loren 1977; Blitz & Thaddeus 1980; Leung & Brown 1977) and have often been interpreted as an indication of collapse of outer cool gas onto a hotter core. This explanation may not hold for the region around AFGL 961 as the dip is blueshifted and since the area over which the dip occurs is much larger than the typical expected size of a collapsing region. A similar phenomenon has also been noticed by Xie (1992) in the Mon R2 core.

We now discuss the observed properties of the globules. Globules 1 and 3 clearly have cometary shapes, while globule 2

appears to be a fragmented extension from globule 1. Near the location of globule 6, Block (1990) identified optically three cometary globules all pointing roughly in the direction of IRS. Possibly due to beam dilution, these cometary globules do not appear distinctly on our CO maps. However, globule 6 is elongated roughly in the same NW-SE direction as the optical cometary globules. A spatial velocity cut through this object along this direction shows a velocity gradient of ~ 0.6 km s^{-1} pc^{-1}.

Globule 1 has been identified optically by Block (1990) and by Sugitani et al. (1991) (object 24 in their catalog). Figure 4 presents a superposition of the CO, ^{13}CO and optical emission from this object. There is a definite correspondence between the region of visible extinction and the ^{13}CO emission. However, the optical size of the globule is significantly smaller than indicated by molecular tracers. Although CO emission is widespread over the optical image of the globule, extending beyond the tail, the ^{13}CO emission is confined to the head of the globule. Figure 5 shows a montage of the CO and ^{13}CO spectra in the head region. The ratio of ^{13}CO to CO antenna temperature increases systematically toward the western boundary of the globule's head. This could indicate a gradient in either temperature or column density (or both). However, since this ratio approaches unity, it is more likely to indicate an enhancement in optical depth in this region just inside the bright rim. The antenna temperature of both the species decreases dramatically in this region which is consistent with the photodissociation expected at the rim.

As noted by Block (1990), the symmetry axis of globule 1 seems to point towards IRS. Figure 6 shows a spatial velocity CO map cutting through globule 1 in this direction ("a" in Fig. 1). The velocity separation of the globule relative to IRS is about 6 km s^{-1}. Within the globule, there is a velocity gradient of about 1.6 km s^{-1} pc^{-1}. We also see a velocity gradient in the opposite direction across the emission associated with IRS of ~ 0.5 km s^{-1} pc^{-1}. A spatial velocity cut along a northwest direction ("b" in Fig. 1) across globules 5, 3, and 1 is shown in Figure 7. The complicated structure of velocity gradients in different globules is apparent in this Figure.

Table 1 summarizes the observed physical properties of the globules. All the globules and clumps appear to be at a V_{LSR} of ~ 9 km s^{-1}. Their sizes vary from 1 to 2 pc; globule 6, however, is the most elongated, having a length of about 5 pc. Assuming CO emission to be optically thick and ^{13}CO to be optically thin, and assuming LTE, we calculate column densities and kinetic temperatures toward the central regions of the globules according to the method of Dickman (1978). The kinetic temperatures T_k listed in Table 1 are estimated from the CO antenna temperature, assuming a beam-filling factor of 1. The column densities listed in Table 1 are the mean values in the central regions of the globules and vary from 1 to 7×10^{21} cm^{-2}. The masses were calculated from the LTE column density in each pixel. With the usual uncertainties associated with the LTE method, the globule masses may be in error by about a factor of 2 (not including the uncertainty in the distance to the Rosette nebula). Additional uncertainty is present for clumps 7 and 8 due to confusion with emission from IRS.

3.2. *IRAS Associations*

As noted by Cox et al. (1990), many of the molecular clumps in the Rosette region are associated with *IRAS* sources. Table 2 lists the *IRAS* sources associated with the objects we have identified. The far-infrared luminosities appearing in Table 2

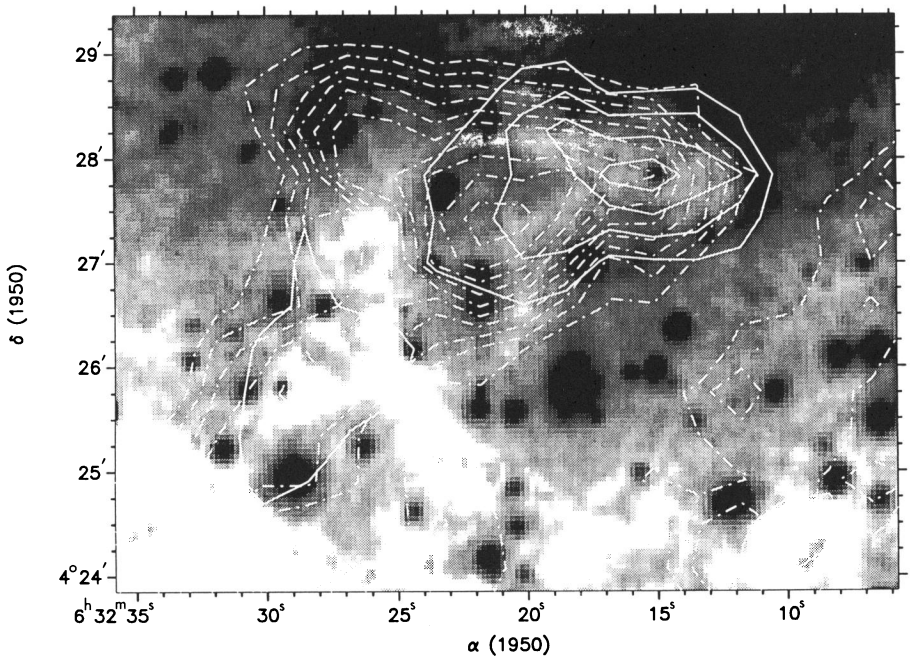

FIG. 4.—Overlay of the optical image of globule 1 with the CO (*dashed contours*) and ^{13}CO (*solid contours*) emission. The CO emission is well confined by the bright rim, showing a sharp decrease in emission at the rim. In the head region there is a clear anticorrelation between the optical and the CO emission, but near the tail the CO emission is extended. ^{13}CO is confined to the head of the globule where the density is presumably enhanced due to the ionization front–driven shock. The embedded *IRAS* source is also faintly visible in this POSS red print, and it is located near the peak of the LTE column density at a distance of about 0.5 pc behind the bright rim on the symmetry axis.

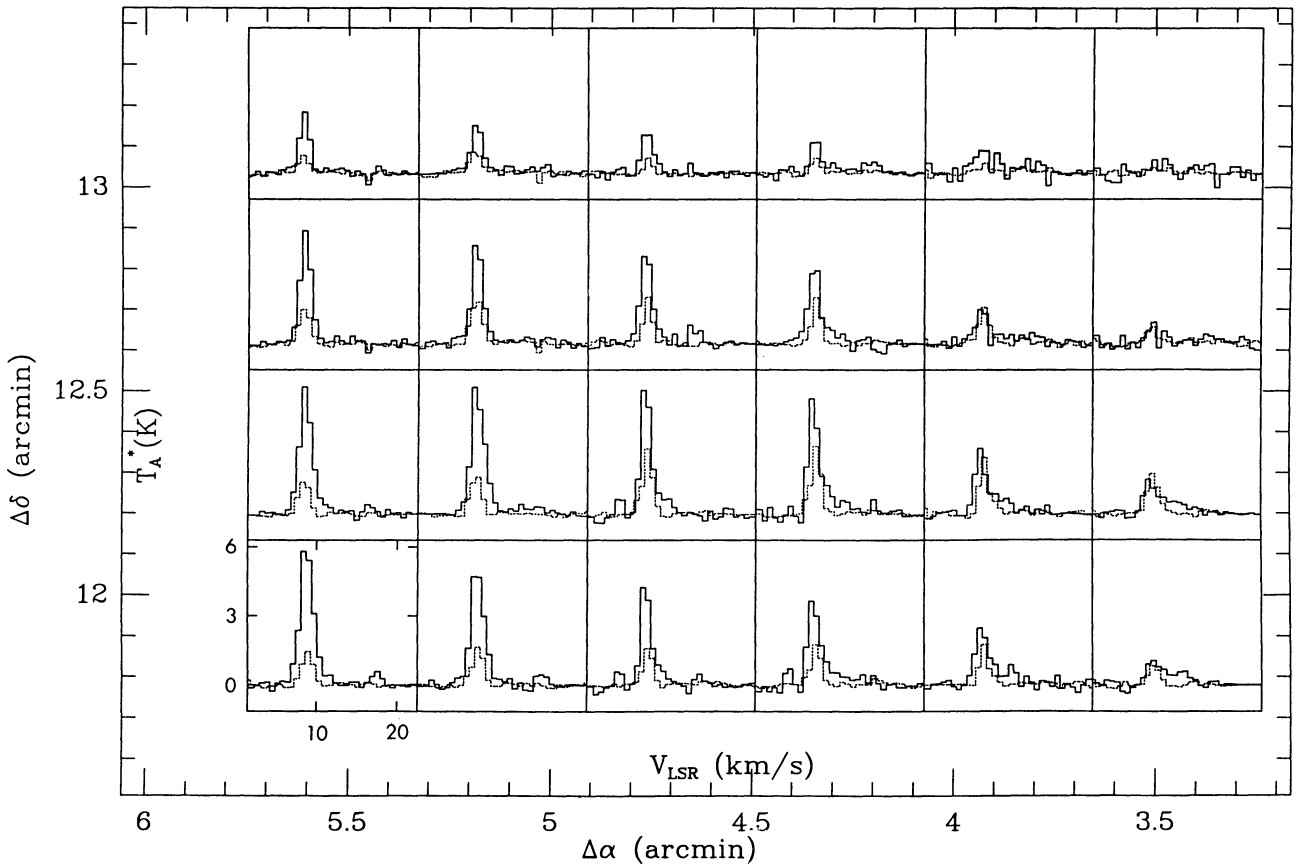

FIG. 5.—Montage of CO (*solid curves*) and ^{13}CO (*broken curves*) spectra in the head region of globule 1. The increasing ratio of ^{13}CO to CO peak intensities toward the direction of the apex at $(\Delta\alpha, \Delta\delta) = (3'.5, 12'.5)$ indicates the increase in column density there due to implosion (offsets measured from AFGL 961, $\alpha[1950] = 06^h31^m58^s$, $\delta[1950] = +04°15'30''$). Near the location of the rim the CO emission decreases sharply, presumably due to photodissociation by the radiation from the H II region which is northwest of the globule.

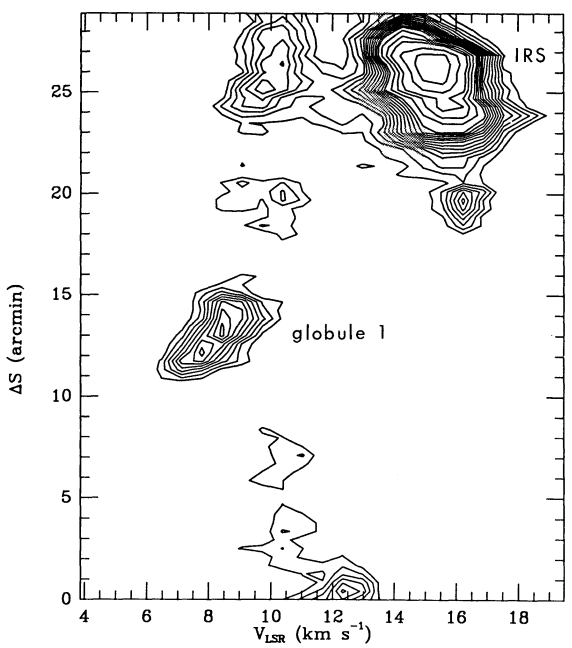

FIG. 6.—Spatial velocity CO map across globule 1 and IRS along the axis indicated as (a) in Fig. 1. The position offset, ΔS, is measured from $(\alpha, \delta) \approx (06^h32^m50^s, 04°28'30'')$. This figure shows that the globule is blueshifted by about 7 km s^{-1} with respect to IRS. There is a velocity gradient of 1.6 km s^{-1} pc^{-1} along the direction pointing toward IRS.

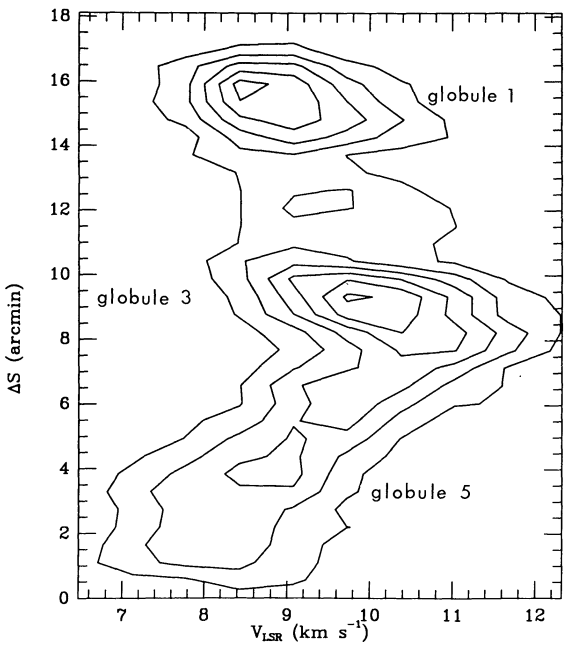

FIG. 7.—Spatial velocity map across globules 1, 3, and 5 along the direction indicated as (b) in Fig. 1, toward the direction of the central stars in NGC 2244. The position offset, ΔS, is measured from $(\alpha, \delta) \approx (6^h33^m, 4°,14')$. The velocity gradients seen across globules 1 and 3 are similar but are of opposite sign from the gradient seen in globule 5.

TABLE 1

PHYSICAL PROPERTIES OF THE GLOBULES

Globule	α(1950)	δ(1950)	T_k (K)	V_{LSR} (km s^{-1})	$N(H_2)$ $\times 10^{21}$ cm^{-2}	Mass ($M_\odot$)	a[a] (pc)	b[a] (pc)	*IRAS* Source
1	06^{h}32^{m}18^s.5	04°27′50″	16.3	8.8	6.8	100	1.4	1.8	06322+0427
2	06 32 28.0	04 25 45	12.3	9.2	1.1	50	0.7	0.8	...
3	06 32 32.0	04 22 24	15.3	9.7	6.6	150	1.8	2.9	06327+0423 X0632+043[b]
4	06 32 31.9	04 22 24	9.3	9.2	1.6	200	1.5	2.7	...
5	06 32 48.6	04 19 53	11.6	9.5	2.2	300	2.3	2.5	...
6	06 32 40.2	04 13 12	11.2	9.1	3.4	200	2.1	4.6	...
7	06 31 40.0	04 20 44	13.5	9.2	22	100	2.1	2.0	06314+0421
8	06 31 33.3	04 26 10	14.7	9.5	11	100	1.9	1.5	...
9	06 31 51.7	04 26 35	11.2	9.2	4.6	50	1.5	1.6	...

[a] a is the diameter along the minor axis, and b, along the major axis.
[b] From *IRAS* Small Scale Structure Catalog.

TABLE 2

IRAS SOURCES ASSOCIATED WITH THE GLOBULES

				Flux (Jy)					
Source	*IRAS*	α(1950)	δ(1950)	12 μm	25 μm	60 μm	100 μm	$L(L_\odot)$	Association
1	06314+0421	06^{h}31^{m}28^s.1	04°21′26″	0.7	1.6	105	323.6	737	Globule 7
2	06314+0427	06 31 26.6	04 27 17	6.1	6.5	129.3	323.6	924	CO peak (IRS)
3	06318+0420	06 31 53.6	04 20 13	1.5	3.8	36.6	995.2	1368	...
4	06319+0415	06 31 59.0	04 15 09	78.4	375.8	958.8	995.2	7622	AFGL 961
5	06322+0427	06 32 16.5	04 27 40	0.4	0.7	10.2	73.9	131	Globule 1
6	06327+0423	06 32 47.0	04 23 13	0.5	0.8	8.2	62.7	114	Globule 3
7	X0632+043	06 32 31.6	04 23 46	...	...	...	299	...	Globule 3

were calculated using the following formula (Casoli et al. 1986),

$$L_{IR} = 4.7 \times 10^{-6} D^2 \left(\frac{S_{12}}{0.79} + \frac{S_{25}}{2} + \frac{S_{60}}{3.9} + \frac{S_{100}}{9.9} \right) L_\odot , \quad (1)$$

where D is the distance in pc and S_λ is the flux density in Jy. In globule 1, IRAS 06322+0427 appears faintly on the POSS red print, at the location of the peak in ^{13}CO emission (see Fig. 4). This source is located at a distance of about 0.5 pc behind the rim. Within the sensitivity of our observations (see Fig. 5), the spectra do not show any indication of an outflow near this *IRAS* source. We have also detected CS $J = 2$–1 emission from the location of this *IRAS* source where it appears to have a peak. This spectrum is shown in Figure 8. Following Goldsmith et al. (1992b), and assuming a value of 10^{-8} for the abundance of CS relative to H_2, we estimate a density of $\sim 8 \times 10^3$ cm^{-3} (averaged over the beam), at this location.

Two *IRAS* sources are found to be associated with globule 3. Of these X0632+043 is from the *IRAS* Small Scale Structure Catalog, and has a relatively large positional uncertainty ($\sim 4'$). Figure 9 is a plot of integrated ^{13}CO emission from globule 3 which shows two peaks in emission separated by ~ 1.5 pc along east-west. IRAS 06314+0421 also appears near the peak in ^{13}CO emission in globule 7. All these *IRAS* point sources have colors which are characteristic of those sources associated with dense cores (Emerson 1987; Parker 1991) and it thus seems plausible that these infrared sources are embedded within the globules.

4. DISCUSSION

Our CO and ^{13}CO mapping has revealed the following distinguishing characteristics of the globules in the SE quadrant of the Rosette nebula: (1) They appear cometary in shape (Figs. 1, 4 and 9); (2) their velocities are blueshifted with respect to the Rosette molecular cloud by about 6 km s^{-1} (Figs. 2 and 3); (3) they have internal velocity gradients (Figs. 6 and 7); and (4) they show signs of star formation as suggested by the presence of *IRAS* point sources at the location of peaks in ^{13}CO emission (Figs. 4 and 9). Globule 1 shows the presence of a bright rim roughly facing NW (Figs. 1 and 4) toward the exciting stars of the NGC 2244 H II region. We now briefly discuss in the context of our observations some of the theoretical models, which are relevant to understanding the structure and origin of these cometary globules.

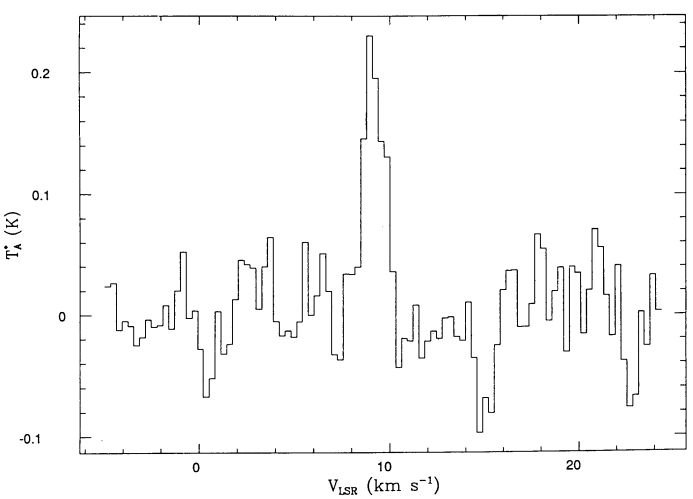

FIG. 8.—CS $J = 2$–1 emission from the location of the *IRAS* source 06322+0427 at the head of globule 1.

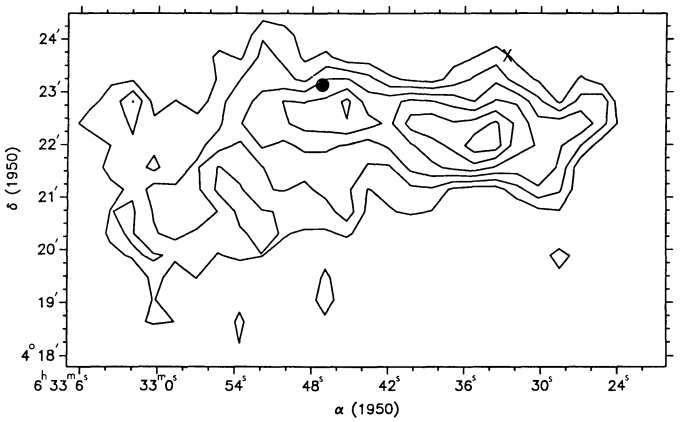

FIG. 9.—Association of *IRAS* sources 06327+0423 (*filled circle*) and X0632+043 (*cross*) with the peaks in ^{13}CO integrated intensity between 9 and 12 km s^{-1} in globule 3. X0632+043 is from the *IRAS* Small Scale Structure Catalog and has a positional uncertainty of about 4′.4. Contour levels are separated by 0.5 K km s^{-1} between 1 and 3.5 K km s^{-1}.

An early idea suggests that cometary globules evolve from elongated protrusions (elephant trunk globules) which are caused by Rayleigh-Taylor instability in a shell of dense gas which is external to and pressurized by hot ionized gas (Pottasch 1958b; Herbig 1974). As shown by Schneps et al. (1980), the elephant trunk globules in the NW quadrant of the Rosette nebula were most likely created by a Rayleigh-Taylor instability. The SE globules discussed here differ in a number of respects from those in the NW quadrant. The SE globules appear to be farther away from the central exciting source of the H II region, while the NW globules project into the H II region from the interface between the H II region and the molecular material. The SE globules lie in a relatively quiescent region and are visible only on enhanced POSS images, while the NW globules appear as silhouettes against the bright Hα emission from the H II region. The globules evolved from the elephant trunks in the NW are typically very small (0.02–0.2 pc), and are referred to as teardrop globules (Herbig 1974; Cernicharo 1991). The sizes of the SE globules are, on the other hand, typically larger than 1 pc (Table 1). If the SE globules were created by Rayleigh-Taylor mechanism, the observed internal velocity gradients should be due to the stretching of the globule, as discussed by Schneps et al. (1980), then the velocity gradients should occur along directions nearly parallel to each other, which is not what is observed (see Figs. 6 and 7). In this scenario, cometary globules are the tips of the inward-projecting tongues of material. As such, they should have a smaller outward velocity (relative to central star of H II region) than the material of the shell at their base. In fact, we see the SE globules in projection against the H II region, but they are blueshifted compared to the extended emission, opposite from what would be expected in this picture. Hence, we feel that the Rayleigh-Taylor mechanism is less likely to be the cause for the globules in the SE quadrant of the Rosette nebula.

Another possibility is that the SE globules have formed from fragmentation of an unstable layer between the ionization front and the shock front at the interface between the neutral and the ionized region (Elmegreen & Lada 1977). If we assume a density of 10^3 cm^{-3} for the molecular cloud, a temperature of 100 K for the cooled, postshock (CPS) layer, and an O star column density of 10 per 100 pc^2, we obtain from equation (13) of Elmegreen & Lada (1977) that the thickness of the CPS layer would be ~0.6 pc at a distance of 25 pc from the central exciting source. This value is considerably smaller than the size of the region occupied by the globules. One may argue that the CPS layer which was fragmented and led to the formation of the globules is almost normal to the line of sight. However, the apparent cometary form of the globules suggests otherwise. The velocity of the shock given by equation (7) of Elmegreen & Lada, for a distance of 25 pc, is 4.2 km s^{-1}. This is comparable to the velocity of the globules with respect to the Rosette molecular complex. According to Elmegreen & Lada, due to the inhomogeneities in the molecular cloud, different parts of the shock will be at different distances from the exciting star with a resulting difference in velocity given by $\Delta v_s/v_s \sim \Delta r/4r$. Using the observed value of the velocity of globules for $v_s \sim$ 6 km s^{-1}, and a typical separation of ~5 pc, we get $\Delta v_s/v_s \sim$ 0.05, which is considerably smaller than the observed velocity spread of ~0.25 as seen from Table 1. With these considerations, while we cannot completely rule out the possibility that the globules have resulted from a CPS layer, the Elmegreen & Lada mechanism is not highly compelling.

An intense flux of UV radiation can cause the implosion of a neutral cloud as studied numerically by Sandford, Whitaker, & Klein (1982) and by Klein et al. (1985). A detailed analytical study of photoevaporating globules has been made by Bertoldi (1989) and Bertoldi & McKee (1990), who also demonstrated the consistency of their theory with the observed parameters of the elephant trunk globules in the northwest quadrant of the Rosette nebula and the cometary globules in the Gum nebula. An application of this theory has also been made recently to an observational study of a bright rim in NGC 2264 by Tauber, Lis, & Goldsmith (1993), who found it to be reasonably consistent with their observations. In the formalism of Bertoldi & McKee (1990), a cloud surviving the UV radiation will settle into an equilibrium cometary configuration in a sound crossing time, while accelerating away from the exciting source. Thus this model appears of considerable interest for understanding the SE globules.

Given that molecular clouds are typically very clumpy (Stutzki et al. 1988; Boissé 1990; Tauber & Goldsmith 1990; Elmegreen 1992), we prefer the interpretation that the cometary globules have evolved from preexisting clumps in the molecular cloud, under the effect of UV radiation from the central OB stars in NGC 2244. Due to clumpiness in the molecular cloud, the ionizing radiation penetrates into the cloud effectively, and reaches the dense clumps in the more distant part of the molecular cloud. The initial conditions in the clumps favor a D-type ionization front which drives a shock inside the clumps which evolve to become globules. These globules subsequently maintain a stationary state in which they appear to have a cometary form. Since the globules appear as enhanced extinction in the optical image, and as their velocities are blueshifted with respect to that of the exciting stars, they are in the foreground and have been accelerated toward us, away from the Rosette molecular cloud. It is likely that globule 2 is a clump that has fragmented from globule 1 due to the radiative implosion. A similar phenomenon is also suggested from the ^{13}CO map of the integrated intensity between 9 and 12 km s^{-1} in globule 3 as shown in Figure 9. The *IRAS* sources 06327+0423 and X0632+043 in globule 3 indicate the possibility of multiple star formation along the symmetry axis of a radiatively imploded globule. In the CO observations of the prominent cometary globule in IC 1396, we

can see a similar fragmentation along the symmetry axis (see Fig. 3*a* of Nakano et al. 1989).

The influence of radiation from NGC 2244 is directly indicated by the presence of the bright rim in globule 1. Another indication of this interaction is seen in a small region that projects out of clump 9 toward the northeast. On the CO spatial velocity map shown in Figure 6, this region appears at $\Delta S \approx 20'$, and the size of this projection is ~ 1 pc. The spectra around this position are shown in Figure 10. We see that the narrow redshifted CO emission (FWHM ~ 1.8 km s^{-1}, at $V_{LSR} \sim 16$ km s^{-1}) occurs in the same region that shows the broad blueshifted emission (FWHM ~ 3 km s^{-1}, at VLSR $\sim$ 8.5 km s^{-1}). The ^{13}CO emission is below the sensitivity of our observations. One possibility is that this clump has been shocked and the post–shock-heated gas is responsible for the broad blueshifted line while the preshocked cooler gas produces the narrower redshifted (or at ambient velocity) emission (a similar example of such a phenomenon has been noted earlier by Wilking et al. 1984 in W5).

Bertoldi (1989) has presented an initial cloud parameter space in terms of cloud column density and a parameter that characterizes the ionization strength. With the source of UV radiation as the central OB stars of NGC 2244 for which the Lyman-continuum photon luminosity is 5.8×10^{49} photons s^{-1} (Cox et al. 1990), and assuming that our measured mean value of column density is representative of the initial value we find that globule 1 lies in region II of Bertoldi's plot of initial cloud parameter space (see Fig. 1 of Bertoldi 1989). This region corresponds to clouds which will be compressed by an ionization front–driven shock, with an ionized gas boundary layer (recombination layer) that is thin compared to the size of the globule. Clouds of these characteristics will be accelerated away from the source of the UV radiation rather than being completely ionized as would occur, for example, for lower mass objects.

Based on the optical morphology of the globules, Block (1990) has suggested that they are largely influenced by stellar winds from a hidden O7 star at the location of IRS. Due to a smaller distance between the globules and this hidden exciting source at IRS, a smaller value of its luminosity corresponding to a single O7 star, $\sim 0.2 \times 10^{49}$ photons s^{-1}, may still produce a flux comparable to that due to the stars in NGC 2244 assuming that the true and projected distances are not very different. However, the spectral type of this hidden object was inferred from the observed far-infrared flux assuming a single source of radiation. Subsequent infrared imaging has revealed the presence of a cluster of objects at this location (Block et al. 1992). This would lead to a smaller value of luminosity for this hidden source. It seems more likely that the globules are primarily affected by the radiation from NGC 2244 and only weakly influenced by the young stellar object(s) at IRS. The clump associated with this object (where the CO emission peaks) also lies in region II of Bertoldi's phase diagram. This supports the possibility that IRS may also be a

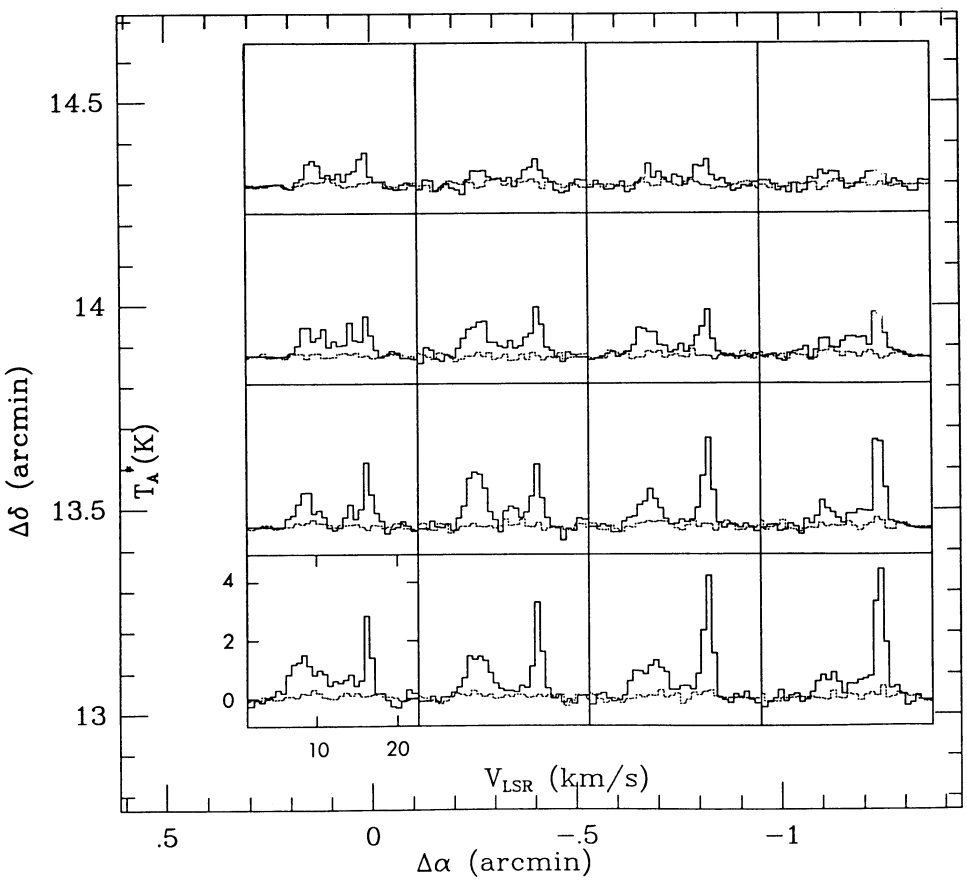

FIG. 10.—CO and ^{13}CO spectra from a region near clump 9, projecting toward the H II region. The narrow CO line represents emission from the preshocked gas that is at the velocity of the Rosette cloud complex, while the postshock heated gas in the clump is responsible for the broad blueshifted line.

result of radiative implosion as suggested earlier by Blitz & Thaddeus (1980).

From equation (3.23) of Bertoldi & McKee (1990), we estimate the pressure due to the hot ionized gas produced by the UV radiation to be 4.1×10^{-10} dyn cm^{-2}, assuming the exciting source to be the stars in NGC 2244. We estimate the internal pressure in the globules from their observed linewidths and find it to be of the order of 10^{-10} dyn cm^{-2}, showing that the globules are likely to be in near pressure equilibrium. The external pressure near the tail region of the globules is expected to be less, and correspondingly these regions in the globules appear more diffuse as seen in Figures 4 and 9. Block (1990) has suggested that the globules are influenced by a stellar wind from a hidden O7 star at the location of IRS. Equation (3.36) of Bertoldi & McKee (1990) gives the ratio of the pressure due to the hot ionized gas to the ram pressure due to the stellar wind from the exciting source. With the exciting source to be the stars in NGC 2244, we find this ratio to be of the order of 3000, while with the exciting source to be a hidden O7 star at the location of IRS, we find this ratio to be about 200. It appears that the stellar wind would have to be unusually strong in order for it to dominate the effect of the UV radiation. However, as seen from Figures 1 and 6, the symmetry axis of globule 1 and the direction of the velocity gradient point towards IRS, suggesting an interaction with the source at this location, but the nature of this interaction remains unclear. Further infrared observations would be helpful to clarify the characteristics of this hidden source.

It is interesting to compare the estimated LTE mass with the virial mass to approximately check if the globules are gravitationally self-bound. Using a value of 0.5 pc for its radius and a ^{13}CO line width of 1.5 km s^{-1}, we find the virial mass of globule 1 to be $\sim 140\ M_\odot$, where we have neglected magnetic field and external pressure, and assumed a variation in density as $1/r^2$ (McLaren, Richardson, & Wolfendale 1988). For the case of constant density and a density variation as $1/r$, we get 236 and 214 $M_\odot$, respectively. These virial mass estimates are greater than or comparable to the 100 $M_\odot$ LTE mass of the globule, suggesting that the globule is at best critically self-bound excluding the effect of the radiative implosion. However, the presence of the *IRAS* source in the head of the globule suggests that collapse has taken place, and thus radiative implosion is likely to have played an important role in star formation in this globule.

The SE globules are observed to have velocities typically 6 km s^{-1} blueshifted relative to the extended emission in the Rosette molecular cloud. The estimated UV flux at globule 1 and its mass from the CO observations, locates it in the equilibrium cometary cloud mass–flux parameter space defined by Bertoldi & McKee (1990) (see their Figs. 13 and 14), in a region which corresponds to the following characteristics: (1) The globule will not be instantly ionized by the radiation; (2) during its initial radiation driven implosion, it will gain a velocity of ~ 2.5 km s^{-1} (eq. [2.5] of Bertoldi 1989); (3) the globule will move far from its initial position while evaporating. Whether this initial velocity increases to a value close to that observed is difficult to ascertain given the uncertainties in the initial conditions. However, it seems plausible that this mechanism described by Bertoldi & McKee can explain the observed velocities of the SE globules.

The dynamical age of the Rosette nebula is about $2–6 \times 10^5$ yr (Mathews 1967). NGC 2244 has two stars with spectral types earlier than O6 which have upper age limits of 3×10^6 yr (Stothers 1972). The dynamical age inferred from the velocity gradient in globule 1 is $\sim 6 \times 10^5$ yr (see Fig. 6). From the velocity gradients in the elephant trunk globules in the northwest quadrant, Schneps et al. (1980) have estimated their age to be $3–5 \times 10^5$ yr. We have assumed that the SE globules have evolved from preexisting clumps under the influence of UV radiation from NGC 2244. We estimate the typical sound crossing time in these clumps to be of the order of 10^7 yr, neglecting magnetic fields and using a size of 1 pc. Using equation (4.10*a*) of Bertoldi & McKee (1990), we find the characteristic evaporation time for globule 1 to be $\sim 4.5 \times 10^7$ yr, somewhat greater than the sound crossing time. However, as noted by Bertoldi & McKee, if the clump is magnetic (with a typical field strength of the order of 30 μG) then the sound crossing time (eq. [4.8] of Bertoldi & McKee) is 3.4×10^5 yr, significantly less than the evaporation time. Hence a magnetic postimplosion clump would have enough time to settle into an equilibrium cometary configuration as described by the formalism of Bertoldi & McKee, within a time scale that is consistent with the dynamical time scale of the Rosette nebula and the age of the O-type stars noted above. Such cometary globules would then also have the consequences of radiative implosion and acceleration away from the source of UV as described by Bertoldi & McKee, with a typical velocity of about 5 km s^{-1}. While a more exact confirmation of the calculations of Bertoldi & McKee (1990) requires further observations, in particular observations of the ionized gas near the bright rim of the globules and observations at higher angular resolution to study the density profiles of the globules, all the major observational features of the globules reported here appear consistent with this model.

5. SUMMARY

Our study of CO and ^{13}CO emission from the newly identified cometary globules in the southeast quadrant of the Rosette nebula has led to the following main results. The globules are kinematically distinct from the Rosette molecular cloud, having a velocity of 6–7 km s^{-1} relative to the stars and ionized gas of the H II region. Two of these globules appear to be examples of star-formation by radiatively driven implosion of molecular clouds and they provide an opportunity to check the theoretically predicted characteristics of clouds influenced by neighboring young stars. These globules appear to have imploded under the influence of ionizing radiation from the OB stars in NGC 2244. A hidden young stellar object at the position of the CO peak may also be affecting the globules as suggested by their orientation and the directions of internal velocity gradients. However, the central stars in NGC 2244 seem to have had a more significant effect on the globules.

We thank Ron Snell and Frank Bertoldi for helpful discussions, and Chris Salter for suggestions on improving the manuscript. We are grateful to K. Sugitani for providing us the optical photograph of the Rosette region. The Five College Radio Astronomy Observatory is operated with the permission of The Metropolitan District Commission. This work was supported in part by NSF grant AST 9115721. This is contribution 791 of the Five College Astronomy Department.

REFERENCES

Bertoldi, F. 1989, ApJ, 346, 735
Bertoldi, F., & McKee, C. F. 1990, ApJ, 354, 529
Blitz, L., & Stark, A. 1986, ApJ, 300, L89
Blitz, L., & Thaddeus, P. 1980, ApJ, 241, 676
Block, D. 1990, Nature, 347, 452
Block, D., Dyson, J. E., & Madsen, C. 1992, ApJ, 390, L13
Boissé, P. 1990, A&A, 228, 483
Casoli, F., Dupraz, C., Gerin, M., Combes, F., & Boulanger, F. 1986, A&A, 169, 281
Celnick, W. E. 1985, A&AS, 53, 403
Cernicharo, J. 1991, in The Physics of Star Formation and Early Stellar Evolution, ed. C. J. Lada & N. D. Kylafis (Dordrecht: Kluwer), 287
Cox, P., Deharveng, L., & Leene, A. 1990, A&A, 230, 181
Dibai, E. A. 1960, Soviet Astr. J., 4, 13
Dickman, R. L. 1978, ApJS, 37, 407
Dickman, R. L., Horvath, M. A., & Margulis, M. 1990, ApJ, 365, 586
Duncan, J. C. 1920, ApJ, 51, 4
Duvert, G., Cernicharo, J., Bachiller, R., & Gomez-Gonzalez, J. 1990, A&A, 233, 190
Elmegreen, B. G. 1992, in Star Formation in Stellar Systems, ed. G. Tenorio-Tagle, M. Prieto, & F. Sanchez (III Canary Islands Winter School on Astrophysics) (Cambridge: Cambridge Univ. Press), 381
Elmegreen, B. G., & Lada, C. J. 1977, ApJ, 214, 725
Emerson, J. P. 1987, in IAU Symp. 115, Star-Forming Regions, ed. M. Peimbert & J. Jugaku (Dordrecht: Reidel), 19
Erickson, N. R., Goldsmith, P. F., Novak, G., Grosslein, R. M., Viscuso, P. J., Erickson, R. B., & Predmore, C. R. 1992, IEEE Trans. Microwave Theory Tech., 40, 1
Falgarone, E., Phillips, T. G., & Walker, C. K. 1991, ApJ, 378, 186
Goldsmith, P. F., Lis, D. C., Lester, D. F., & Harvey, P. M. 1992a, ApJ, 389, 338
Goldsmith, P. F., Margulis, M., Snell, R. L., & Fukui, Y. 1992b, ApJ, 385, 522
Harju, J., Sahu, M., Henkel, C., Wilson, T. L., Sahu, K. C., & Pottasch, S. R. 1990, A&A, 233, 197
Herbig, G. H. 1974, PASP, 86, 604
Klein, R. I., Whitaker, R. W., & Sandford, M. T. 1985 in Protostars and Planets II, ed. D. Black & M. Matthews (Tucson: Univ. of Arizona Press), 340
Kuchar, T., Blitz, L., & Bania, T. M. 1993, in preparation
Leung, C. M. 1985, in Protostars and Planets II, ed. D. Black & M. Matthews (Tucson: Univ. of Arizona Press), 104
Leung, C. M., & Brown, R. L. 1977, ApJ, 214, L73
Mathews, W. G. 1967, ApJ, 147, 965
McLaren, I., Richardson, K. M., & Wolfendale, A. W. 1988, ApJ, 333, 821
Nakano, M., Tomita, Y., Ohtani, H., Ogura, K., & Sofue, Y. 1989, PASJ, 41, 1073
Osterbrock, D. E. 1957, ApJ, 125, 622
Parker, N. D. 1991, MNRAS, 251, 63
Pottasch, S. 1956, Bull. Astron. Inst. Netherlands, 13, 77
———. 1958a, Bull. Astron. Inst. Netherlands, 14, 29
———. 1958b, Rev. Mod. Phys., 30, 1053
Reipurth, B. 1983, A&A, 17, 183
Sahu, M., Pottasch, S. R., Sahu, K. C., Wesselius, P. R., & Desai, J. N. 1988, A&A, 195, 269
Sandford, M. T., Whitaker, R. W., & Klein, R. I. 1982, ApJ, 260, 183
Schneider, S., & Elmegreen, B. 1979, ApJS, 41, 87
Schneps, M. H., Ho, P. T. P., & Barrett, A. H. 1980, ApJ, 240, 84
Serabyn, E., Güsten, R., & Mundy, L. 1993, ApJ, 404, 247
Snell, R. L., & Loren, R. B. 1977, ApJ, 211, 122
Sridharan, T. K. 1992, J. Astrophys. Astron., 13, 217
Stothers, R. 1972, ApJ, 175, 431
Stutzki, J., Stacey, G. J., Genzel, R., Harris, A. I., Jaffe, D. T., & Lugten, J. B. 1988, ApJ, 332, 379
Sugitani, K., Fukui, Y., Mizuro, A., & Oshashi, N. 1989, ApJ, 342, 47
Sugitani, K., Fukui, Y., & Ogura, K. 1991, ApJS, 77, 59
Tauber, J. A., & Goldsmith, P. F. 1990, ApJ, 356, L63
Tauber, J. A., Lis, D., & Goldsmith, P. F. 1993, ApJ, 403, 202
Turner, D. G. 1976, ApJ, 210, 65
Wilking, B. A., Harvey, P. M., Lada, C. J., Joy, M., & Doering, C. R. 1984, ApJ, 279, 291
Wootten, A., Sargent, A., Knapp, G., & Huggins, P. J. 1983, ApJ, 269, 147
Xie, T. 1992, Ph.D. thesis, Univ. of Massachusetts